

## Fabrication of polysulfone/chitosan composite membrane with various concentrations of polysulfone

Norin Zamiah Kassim Shaari\*, Mohammad Najib Mohamad Ishak, Nurul Aida Sulaiman

Faculty of Chemical Engineering, Universiti Teknologi MARA, Selangor, Malaysia

\*Corresponding email: [norinzamiah@uitm.edu.my](mailto:norinzamiah@uitm.edu.my)

### Abstract

In this study, a thin film composite (TFC) membrane was fabricated by using polysulfone (PSF) membrane as a supporting layer and hybrid membrane as a barrier layer. The PSF membranes were prepared by using phase inversion method while the hybrid membranes were formulated from polymer blend of chitosan (CS)/polyethylene glycol (PEG) and cross linked with tetraethylorthosilicate (TEOS). The aim of this work is to study the effects of varying the PSF concentrations on the characterisation and performance of the TFC membranes. Three different PSF concentrations were selected; 11 wt.%, 13 wt.%, and 15 wt.%. The TFC membrane was characterised by using attenuated total reflectance Fourier transform infrared (ATR-FTIR) spectroscopy and thermogravimetric analysis (TGA). In the performance testing, pure water permeability (PWP) was conducted to measure water flux, and antifouling experiment by using humic acid and deionised water as feed solution was carried out. Results show that TFC membrane with 11 wt.% PSF has excellent membrane characteristics and performance. This membrane shows better water permeation, and has antifouling properties, which was exhibited through high relative flux recovery (RFR) and low relative flux decay (RFD) as compared to other membranes. This fabricated membrane has potential to be used in wastewater treatment highlight the most significant findings or observations that would attract attention of readers.

### Article Info

*Article history:*

Received date: 24 March 2019

Accepted date: 26 April 2019

*Keywords:*

Thin film composite  
PSF/CS membrane  
Antifouling  
Pure water flux  
Humic acid

### 1.0 Introduction

Industrial effluents contain high amount of harmful materials such as heavy metals, oil, and other contaminants. These harmful and toxic materials can affect the receiving water, pollute the environment, endangers human life and aquatic life if they are not being treated effectively. Heavy metal is known to be non-biodegradable, toxic, and carcinogenic. Soluble and emulsified oil in wastewater is difficult to be treated by traditional methods (Zhang et al, 2010).

Membrane processes have attracted an increasing attention in the last few years. It is widely used in food, drug and chemical industries, wastewater treatment, purification of water, water desalination, and separation processes. Membrane processes also have many advantages such as cost and space savings, easy in operation, high efficiency, and capability to reduce contaminants (Kumar et al, 2013a).

Therefore, effective removal of heavy contaminants by membrane separation process is important to protect the environment as well as human and aquatic life. The membrane processes that are widely used in wastewater

treatment including ultrafiltration, reverse osmosis, nanofiltration, and electrodialysis. In order to achieve an excellent membrane separation process, both hydrophilicity and porous structure of the membrane play important roles. Moreover, excellent chemical resistance towards the composition and pH of feed solution, good thermal stability, and porous structure could lead to the increase in the membrane permeation (Kumar et al, 2013b).

Polysulfone (PSF) membrane, which is made by phase inversion method, becomes an outstanding ultrafiltration membrane material due to its flexibility, good oxidative stability, thermal stability, and hydrolytic stability. Furthermore, this polymer has good mechanical, electrical, chemical, and aging resistance properties. Besides its reasonable price, it also has good resistance to extreme pH and temperature, and good in mechanical and film forming properties. It is also widely used in microfiltration and nanofiltration applications where pore sizes would be tailor-made. However, this polymer is hydrophobic in nature that will affect the PSF performance in permeation and antifouling properties. Generally, low antifouling property of the PSF is caused

by its surface hydrophobicity and the low permeability is caused by small pore size, low porosity, and surface hydrophobicity (Kumar et al, 2013c).

Chitosan (CS) is a partially deacetylated polymer of chitin, found in a variety of natural resources including shrimp and crab shells (Smitha et al, 2008). It is biodegradable and biocompatible, antimicrobial, non-toxic, excellent film forming nature, highly selective and hydrophilic, and environmental-friendly (Sangeetha et al, 2016). CS contains amino and hydroxyl groups on its chains which serve as coordination sites and good complexation material to be used as a suitable sorbent for heavy metal ions where it can separate and adsorb a wide range of contaminants including heavy metals. CS is widely used in separation processes such as nanofiltration, ultrafiltration, and reverse osmosis. However, the disadvantages of this polymer are low mechanical stability and insolubility in most common organic solvents, thus, makes it difficult to blend with other polymers in organic solvents (Ghaee et al, 2013). Therefore, in this current study, it is blended with polyethylene glycol (PEG). PEG has high biocompatibility, minimal toxicity and good solubility. Its high hydrophilicity and flexibility can therefore improve the adsorption properties of chitosan (Wang & Kuo, 2007).

Although both CS and PSF polymers have different characteristics, they are good candidates for composite membrane. CS provides the separation/conducting properties, increasing hydrophilicity of the membrane while PSF ensures the structural stability of the composite blend (Smitha et al, 2008). Tetraethylorthosilicate (TEOS) as a cross-linker could control the hydrophilicity of the membrane.

Hamzah et al. (2014) reported that polysulfone concentration has an effect to the performance of the resultant membrane. Therefore, the aim of this work is to identify the optimum PSF concentration that can enhance the performance of the CS/PEG/PSF composite membrane.

## 2.0 Methodology

### 2.1 Materials

The materials used in this experiment include chitosan powder (MW 100,000–300,000) which was purchased from Acros Organics, polysulfone beads (MW 44,000–53,000), polyethylene glycol (MW 1500), hydrochloric acid (purity 37%) and tetraethylorthosilicate (purity 98%), which were purchased from Sigma Aldrich. N-methyl pyrrolidone

(purity 99%) and aqueous acetic acid solution were purchased from Merck Malaysia.

### 2.2 Preparation of PSF membrane

An amount of 11 g PSF beads was first dissolved in 89 mL NMP to produce 11 wt.% of PSF solution. The solution was stirred at 60 °C and 500 rpm for 4 hours (Kumar et al., 2013d). Then, 2 mL of PSF solution was poured onto a glass plate. A bar applicator with the setting thickness of 90 µm was used to form the membrane (Wang & Kuo, 2007). The glass plate was immersed in tap water overnight at room temperature to remove any residual solvent. Then, the membrane film was sun-dried for 24 hours (Kumar et al., 2014). The same steps were repeated to produce 13 wt.% and 15 wt.% of PSF solution, respectively. Table 1 shows the formulations of these solutions.

**Table 1:** Summary of PSF solution preparation

Membrane	PSF (wt.%)	NMP (mL)
M1	11	89
M2	13	87
M3	15	85

### 2.3 Preparation of hybrid solution

An amount of 0.6 g of CS powder was dissolved in 2 wt.% acetic acid solution at room temperature and followed by continuous stirring at 400 rpm. Then 0.3 g PEG was added into the solution based on 2:1 mass ratio CS/PEG at 80 °C and continuously stirred at 500 rpm for 4 hours (Wang & Hon, 2004). The solution was cooled down at room temperature then 3 wt.% TEOS and 1 wt.% hydrochloric acid were added to the solution and it was continuously stirred at 300 rpm for 10 hours, where the temperature was maintained at 30 °C (Sangeetha et al., 2016).

### 2.4 Preparation of thin film composite (TFC) membrane

About 4 to 5 drops of hybrid solution were poured and a glass rod was used to coat the surface of each PSF membrane uniformly. The membranes were left to dry at room temperature for 1 day. The membranes were then heat-cured in the oven at 45 °C for 1 hour (Hamzah et al., 2014).

## 2.5 TFC membrane characterisation

### 2.5.1 Fourier transform infrared spectroscopy (FTIR)

FTIR spectra were used to identify the presence of functional groups and the types of bonding in the thin film composite membrane. The membrane sample was cut into small pieces and placed on the diamond crystal plate of the ATR-FTIR. Prior to the analysis, the plate was cleaned by acetone. The pressure was set to 60–70 N by adjusting the swivel pressure tower and the spectra were collected in the range of 400 to 4000  $\text{cm}^{-1}$  (Kumar et al., 2013d).

### 2.5.2 Thermogravimetric analysis (TGA)

TGA was used to investigate the thermal decomposition behaviour and stability of the membrane. This equipment also detects the weight loss of material as a function of temperature. The samples were cut into tiny pieces, which weighed about 5 to 10 mg for analysis. The samples were then heated at 30 to 900  $^{\circ}\text{C}$  at a heating rate of 10  $^{\circ}\text{C}/\text{min}$  under nitrogen gas (Ghaee et al., 2013).

## 2.6 TFC membrane performance testing

### 2.6.1 Pure water permeability (PWP)

PWP was used to identify the water flux. The apparatus used was dead-end filtration mode of membrane testing rig. The membrane sample was cut into a round shape with a surface area 19.63  $\text{cm}^2$  and placed in the sample section. About 200 mL deionised water was poured into the stainless-steel filtration cell. The measurement was conducted at room temperature and 4 bar pressure was applied by using nitrogen gas. The permeate sample was collected in a beaker. The volume was collected at each 15 minutes time interval then the permeate flux,  $J$  ( $\text{mL}/\text{cm}^2 \cdot \text{min}^{-1}$ ) was calculated by using Eq. (1) (Kumar et al., 2013c).

$$J = \frac{\Delta V}{A \cdot \Delta t} \quad (1)$$

where  $\Delta V$  (mL) is the volume of the permeate sample,  $A$  is an effective membrane area in  $\text{cm}^2$ ,  $\Delta t$  is the permeation time.

### 2.6.2 Antifouling properties

For this performance test, humic acid solution was prepared by dissolving 10 g of humic acid in 500 ppm NaOH solution in the 1L volumetric flask and stored in a sterile glass bottle at 5  $^{\circ}\text{C}$ . Humic acid was used as foulant model to simulate the actual wastewater, which contains organic matters. The equipment used for pure

water permeability test was also used for the antifouling experiment. The filtration processes were divided into 3 stages. Deionised water was used as feed solution and the stabilised flux was recorded for 30 minutes and was denoted as  $J_0$ . The membrane was tested with humic acid solution for 2 hours and the permeate was collected at every 30 minutes interval and recorded versus filtration time. The permeate flux was denoted as  $J_p$ . The membrane was then cleaned by back-washing method. The back-washing method was conducted by immersing the membrane in 20 mL deionised water and stirred in a shaker at 200 rpm for 30 minutes. Deionised water was used again as feed solution and the permeate flux was recorded again for 30 minutes and the final flux was denoted as  $J_1$ . The data were collected to calculate the relative flux decay (RFD) and relative flux recovery (RFR) based on Eq. (2) and (3), respectively (Hamzah et al., 2014).

$$RFD = \left[ \frac{(J_0 - J_p)}{J_0} \right] \times 100 \quad (2)$$

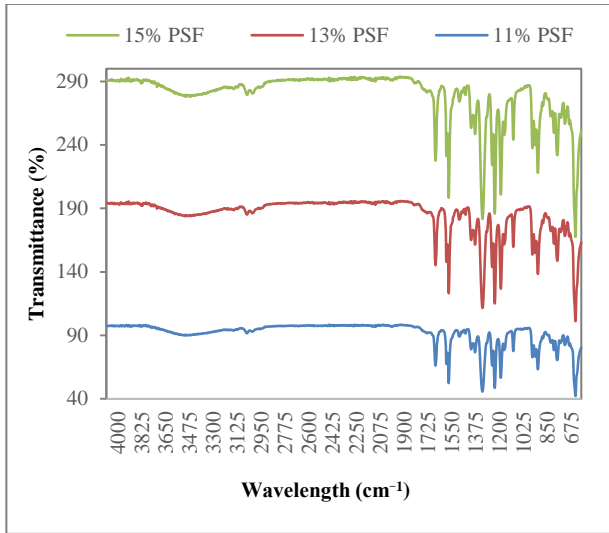
$$RFR = \left[ \left( \frac{J_1}{J_0} \right) \right] \times 100 \quad (3)$$

## 3.0 Results and Discussion

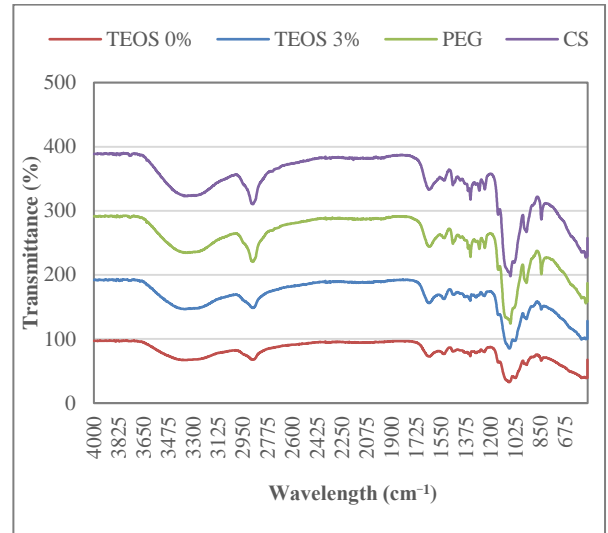
### 3.1 Attenuated total reflectance Fourier transform infrared (ATR-FTIR) spectroscopy

Fig. 1 shows the FTIR spectra of thin film composites with different PSF concentrations. All of the membranes exhibit similar IR spectra. The presence of O–H stretch peak at 3423.75  $\text{cm}^{-1}$  (PSF 11%), 3379.90  $\text{cm}^{-1}$  (PSF 13%), and 3423.90  $\text{cm}^{-1}$  (PSF 15%) are anticipated due to incomplete drying process. Besides that, functional group C=OH also can be represented by peak at 1410.11  $\text{cm}^{-1}$  (PSF 11%), 1409.86  $\text{cm}^{-1}$  (PSF 13%), and 1409.94  $\text{cm}^{-1}$  (PSF 15%) (Padaki et al., 2012). All of the film composites show a peak at 1585  $\text{cm}^{-1}$  corresponding to C=C ring stretch while peaks at 1515, 1150, and 1105  $\text{cm}^{-1}$  indicating C–O–C stretch (Kumar et al., 2013d). Aromatic C=C ring stretch at 1585  $\text{cm}^{-1}$  of each membrane is due to conjugation system of benzene ring (Kumar et al., 2013c). Absorption peaks at 1240 and 557  $\text{cm}^{-1}$  of each membrane show that they have O=S=O functional group which corresponds to symmetric and asymmetric stretching of sulfonated group (Ng et al., 2011).

Fig. 2 shows the ATR-FTIR spectra for pure CS, pure PEG and hybrid solution. The peaks at 3330  $\text{cm}^{-1}$  of each sample represents the O–H stretch while a peak at 2875



**Fig. 1:** ATR-FTIR spectra for 11%, 13% and 15% PSF membranes



**Fig. 2:** ATR-FTIR spectra for hybrid solution, chitosan and polyethylene glycol

$\text{cm}^{-1}$  corresponds to the amide group (Padaki et al., 2012). This amide group will shift to a lower wavenumber caused by cross linking of chitosan chains (Smitha et al., 2008).

But, it is clearly observed that the peak of membrane from CS/PEG polymer blend has the smallest peak due to absence of the TEOS that acts as a cross-linker. For both hybrid solutions, a peak at  $1635 \text{ cm}^{-1}$  corresponds to C-OH functional group (Kumar et al., 2013c). Without TEOS, the membranes have extra functional groups which are C=C and N-H groups at  $1302.85 \text{ cm}^{-1}$  and  $1242.54 \text{ cm}^{-1}$ , respectively (Kumar et al., 2013a). Peaks at  $993$  to  $1090 \text{ cm}^{-1}$  correspond to C-O-C for membranes without TEOS and Si-O-C for hybrid membrane, which resulted from cross linking reaction of polymer blend CS/PEG with TEOS. It is observed that the peak becomes broad with the incorporation of TEOS (Padaki et al., 2012).

### 3.2 Thermogravimetric analysis (TGA)

Fig. 3 shows the percentage of weight residue against temperature for PSF membranes with different polymer concentrations. All membranes show quite similar curves. However, the membrane with 11% PSF has slightly lower thermal stability as compared to other membranes. About 10% average weight loss are observed for all membranes before an excellent thermal stability up to  $480 \text{ }^\circ\text{C}$  is achieved (Suleman et al., 2016). The PSF decomposition starts at  $483.71 \text{ }^\circ\text{C}$  with a huge decrease in weight (Ghaee et al., 2013). This result was anticipated as an increase in temperature will weaken the intermolecular chains between polymer molecules in the membrane resulting

in decrement of mechanical and thermal strength of the polymer (Huang et al., 2018).

As shown in Fig. 4, unlike the polysulfone, hybrid membrane shows three weight loss profiles. Weight loss starts at temperature  $53 \text{ }^\circ\text{C}$  with average 22% is lost due to evaporation of adsorbed and bound water from membrane phase (Huang et al., 2018). The second weight loss at  $183\text{--}287 \text{ }^\circ\text{C}$  corresponds to decomposition of the bound functional groups and the last weight loss represents decomposition of polymer backbone (Jyothi et al., 2018). Decomposition of chitosan starts at  $200 \text{ }^\circ\text{C}$ , whereas the weight loss at  $350 \text{ }^\circ\text{C}$  is due to the decomposition of polyethylene glycol (Ghaee et al., 2013).

### 3.3 Pure water permeability (PWP)

Fig. 5 shows the average water flux for thin film composite membranes with different PSF concentrations. As time increases, the flux decreases for all membrane samples. Flux was taken after 15 min and it was observed that the flux were  $10.45 \text{ L/m}^2\cdot\text{h}$ ,  $23.21 \text{ L/m}^2\cdot\text{h}$  and  $26.36 \text{ L/m}^2\cdot\text{h}$  for PSF 15%, 13% and 11%, respectively. For PSF 11% and 15%, a slow decline in water flux is observed where the average difference between initial and final water flux for both PSF membrane samples is  $6 \text{ L/m}^2\cdot\text{h}$ . However, for PSF 13%, in the first 30 minutes, the water flux decreases rapidly and becomes slower in the last 30 minutes. The average difference between initial and final water flux for PSF 13% membrane samples is  $15 \text{ L/m}^2\cdot\text{h}$ . (Chong et al., 2018).

PWP was applied on the thin film composite membranes to determine the membrane porosity and identify the membrane stability by measuring the water

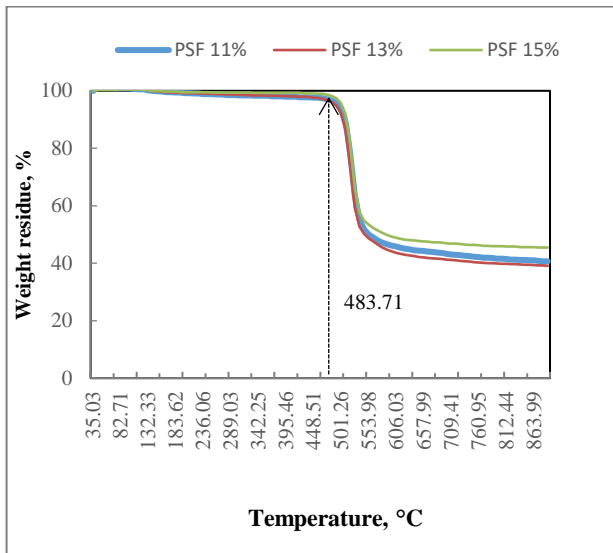


Fig. 3: TGA curves for PSF membrane with different PSF concentrations

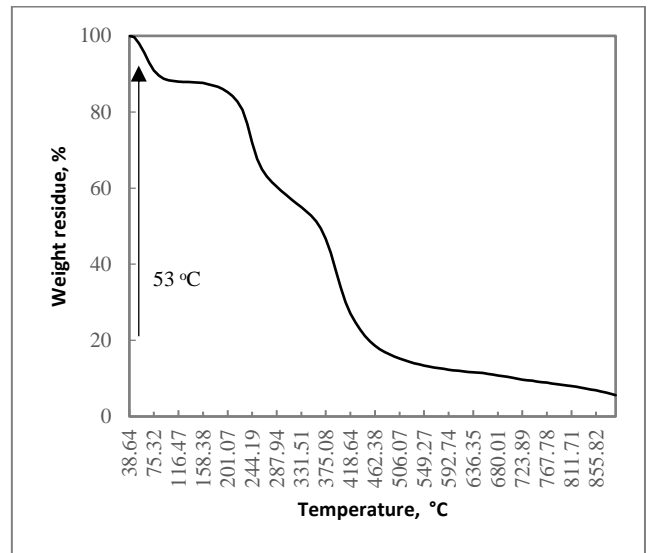


Fig. 4: TGA curve for hybrid membrane

permeability. High permeability indicates high porosity of a membrane. Based on Fig.5, the TFC membrane with PSF 11% shows the highest permeability whereas membrane PSF 15% has the lowest water permeability. Porosity of a membrane also depends on the membrane thickness. This indicates that low polymer concentration produces a thinner and porous membrane thus provides a good hydraulic permeability. These results are in agreement with previous studies which reported that as the polymer concentration increases, the flux and the permeability rates decreases (Ravishankar et al., 2018). On the other hand, as the polymer concentration is increasing, the thickness of the membrane increases causing the membrane to become denser, thus, reduces the rate of water permeability through the membrane due to presence of sponge-like structure (Hamzah et al, 2014).

Membrane pores can be clogged due to particles size is smaller than the pore size. These clogged particles will reduce the membrane flux. From Fig.5, this mechanism can be seen for all membrane samples where the water flux decreases in each interval for 1 hour filtration time. Ravishankar et al. (2018) reported that membrane which had small uniform cylindrical pore configuration can reduce fouling due to difficulty of particles to deposit inside the pores whereas membrane which had sponge-like microstructure could lead to membrane fouling due to porous network of the membrane (Ravishankar et al., 2018). In another research by Kumar et al. (2014), it was reported that the water flux declined with time which was due to accumulation of particles and ions in the pores or on the surface of the membranes.

High PSF concentration will increase the viscosity of the polymer solution which inhibits the growth of

membrane pores. Furthermore, the increase in PSF concentration also increases the hydrophobicity of the membrane which leads to accumulation of particles on the membrane surface (Ariono et al., 2017).

As shown in Fig. 5, it can be observed that there is a decline in water flux between 0.25 to 0.5 hours for all membranes. This phenomenon is due to membrane compaction with the presence of pressure, which compresses the base membrane resulting in partial blocking of pores. However, a steady value of water flux is obtained after 30 minutes of membrane compaction (Kumar et al., 2013b). The initial flux decline also occurs due to mechanical deposition or adsorption of polymeric molecules on the surface of the membranes (Kumar et al., 2013c).

As the water flux depends on the pore size and surface hydrophilicity of the membrane, the presence of CS and PEG on the surface of the PSF membrane has increased the hydrophilicity of the membrane which will lead to an increase in pure water permeability (Kumar et al., 2013a). In contrast, the increase in PSF concentration will increase the hydrophobicity of the membrane.

### 3.4 Antifouling properties

In industrial applications, membrane filtration must have a long-term performance stability and antifouling property to reduce the production cost by reducing the cleaning frequencies and decreasing the energy consumption (Huang et al., 2018). This is because during filtration process, membrane fouling may occur due to hydrophobic interaction between solute and membrane surface where solute is adsorbed and deposited inside membrane pores or on the membrane surface leading to

pore blocking and cake layer growth (Kumar et al., 2014).

These mechanisms are caused by several factors such as hydrophilicity, wettability, surface roughness and surface potential (Kumar et al., 2013d). Antifouling property of the membrane can be increased by reducing surface roughness of the supporting layer of the membrane. Furthermore, high surface roughness reduces the surface porosity, pore size and consequently decreases the flux due to solute is deposited and accumulated in the valleys of the surface roughness (Fang et al., 2018).

Fig. 6 shows the average flux of thin film composites with different PSF concentrations using humic acid solution as a foulant model. The flux decreases with time for all of the membranes due to concentration polarisation and membrane fouling (Guo et al., 2018). The solute molecules are trapped and aggregated on membrane surface and pores caused by strong hydrophobic interaction which generates a fouling layer (Lu et al., 2018). It is observed that the membrane with 11% PSF concentration has the highest average flux in each time interval as compared to the other membranes (13% and 15%) due to high porosity which can reduce the amount of solute accumulation on membrane surface (Hamzah et al., 2014). Generally, the increase in polymer concentration reduces the porosity and pore size thus will cause deposition or adsorption of solute on the membrane surface and produces solute accumulation on the surface and inside the pores (Zhang et al., 2018). Higher polymer concentration especially polysulfone also increases the hydrophobicity of the membrane thus

increases the hydrophobic interaction between solute and membrane surface (Xu et al., 2018).

Fig. 6 also depicts a sharp flux decline for all membranes when humic acid solution replaces deionised water as the feed solution. This phenomena is caused by the composition of the humic acid, where adsorption and deposition of solute molecules from humic acid solution occurs inside the membrane pores and on the membrane surface (Zhang et al., 2018), and further flux decline for 2 hours of humic acid filtration due to formation of a cake layer on the membrane surface (Huang et al., 2018).

Relative flux recovery (RFR) and relative flux decay (RFD) were determined to identify the antifouling property of the membrane. High value of RFR and low value of RFD indicate high efficiency of hydraulic cleaning and good fouling resistant ability and vice versa (Lin et al., 2018). There are two fouling ratios to measure the total fouling which are reversible and irreversible. Reversible fouling ratio occurs from weak interaction between solute and membrane surface which can be eliminated by physical cleaning such as backwashing through hydraulic cleaning or by a strong shear force while irreversible fouling ratio is caused by strong interaction between solute and membrane surface forming a permanent fouling layer, which may be cleaned out by enzymatic degradation or chemical cleaning (Khan et al., 2018).

From Table 1 and 2, TFC membrane with 11 wt. % PSF concentration has the highest RFR value (71.43%) and lowest RFD value (74.14%) followed by 13% PSF concentration (RFR = 64.95%) and (RFD = 84.89%)

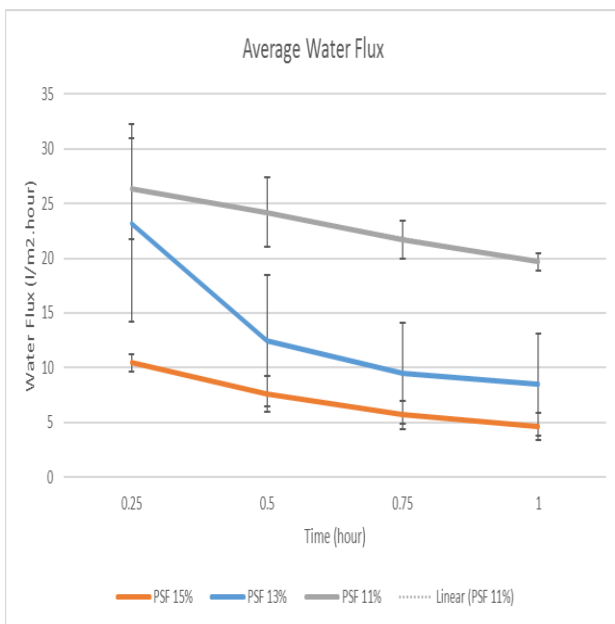


Fig. 5: Average water flux for TFC membranes with different PSF concentrations

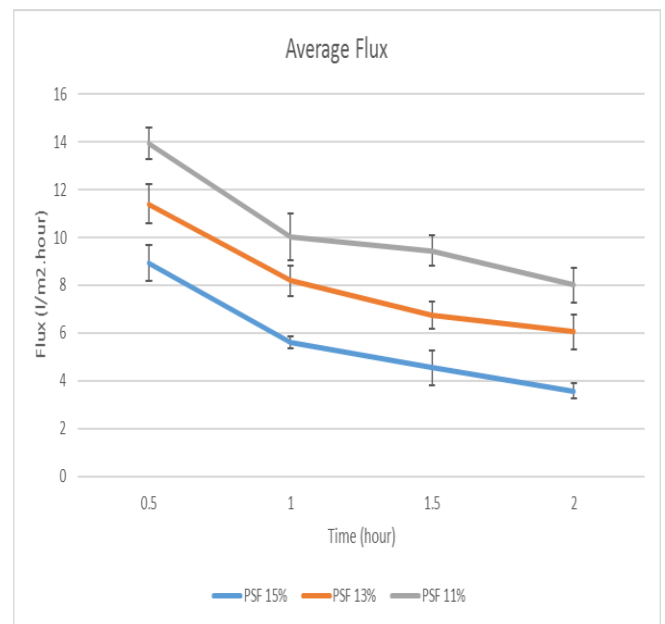


Fig. 6: Average flux for TFC membranes with different PSF concentrations

while the membrane with 15% PSF concentration has the lowest RFR value (68.42%) and highest RFD value (85.52%). These results indicate that solute adsorbed and deposited on the membrane surface of 11 wt.% PSF concentration is easily removed by hydraulic cleaning and remarkably improves the fouling resistant property (Huang et al., 2018). Besides, greater flux recovery occurs due to high reversible fouling ratio which can be restored by hydraulic cleaning compared to irreversible fouling (Khan et al., 2018). However, high flux decay occurs due to a high irreversible fouling ratio where the solute is permanently adsorbed or deposited caused by strong hydrophobic interaction and cannot be restored by hydraulic cleaning (Lu et al., 2018).

**Table 1:** RFR for TFC membranes with different PSF concentrations

PSF concentration %	RFR
15	68.421
13	64.949
11	71.429

**Table 2:** RFD for TFC membranes with different PSF concentrations

PSF concentration %	RFD
15	85.515
13	84.895
11	74.145

The presence of both CS and PEG increases the hydrophilicity of the membrane. These organic polymers reduce the formation of cake layer on the membrane surface. Moreover, smooth membrane with high hydrophilicity can reduce the adhesion of cake layer on membrane surface and may contribute to antifouling performance (Guo et al., 2018). In addition, high CS and PEG and low in PSF concentration can contribute to higher hydrophilicity, which increases the unique water-bounding ability and a thicker the hydration layer on the membrane surface (Zhang et al., 2018). Generally, hydrophilicity will produce molecule-resistant surface which prevents molecules from binding to surface due to strongly bound water molecules (Kumar et al., 2013a).

#### 4.0 Conclusion

This study successfully fabricated TFC membranes by applying phase inversion method. TFC with 11 wt.% PSF exhibited greater flux rate and good anti fouling properties, which was shown by high value of

RFR and low value of RFD. The fabricated membrane has high hydrophilicity, porosity and pore size, which reduces the clogging and accumulation of solutes inside the membrane pores and on the membrane surface resulting in excellent membrane performances. Membrane hydrophilicity also increases with the presence of both CS and PEG that are hydrophilic in nature. In conclusion, thin film composite from hybrid membrane of CS/PEG/TEOS and polysulfone has potential to be used for wastewater treatment.

#### Acknowledgement

The authors gratefully thank UiTM for sponsoring the research through Bestari Perdana grant (600-IRMI/DANA 5/3/BESTARI (P) (009/2018)).

#### References

- A. Ghaee, M. Shariaty-Niassar, J. Barzin, A.F. Ismail, (2013). Chitosan/polyetgersulfone composite nanofiltration membrane for industrial wastewater treatment. *Int. J. Nanosci. Nanotechnol.*, 213-220.
- A. Khan, T. A. Sherazi, Y. Khan, S. Li, S. A. R. Naqvi, Z. Cui, (2018). Fabrication and characterisation of polysulfone/modified nanocarbon black composite antifouling ultrafiltration membranes. *Journal of Membrane Science*, 71-82.
- B. Smitha, D. Anjali Devi, S. Sridhar, (2008). Proton-conducting composite membranes of chitosan and sulfonated polysulfone for fuel cell application. *Journal of Polymer Science*, 4138-4146.
- D. Ariono, P.T.P. Aryanti, S. Subagjo, I.G. Wenten, (2017). The Effect of Polymer Concentration on Flux Stability of Polysulfone Membrane. *AIP Conference Proceedings*, 1-10.
- D. Y. Zhang, Q. Hao, J. Liu, Y. S. Shi, J. Zhu, L. Su, Y. Wang, (2018). Antifouling polyimide membrane with grafted silver nanoparticles and zwitterion. *Separation and Purification Technology*, 230-239.
- H. Guo, Z. Yao, J. Wang, Z. Yang, X. Ma, C. Y. Tang, (2018). Polydopamine coating on a thin film composite forward osmosis membrane for enhanced mass transport and antifouling performance. *Journal of Membrane Science*, 234-242.
- H. Huang, J. Yu, H. Guo, Y. Shen, F. Yang, H. Wang, R. Liu, Y. Liu, (2018). Improved antifouling performance of ultrafiltration membrane via preparing novel zwitterionic polyimide. *Applied Surface Science*, 38-47.
- H. Ravishankar, F. Roddick, D. Navaratn, V. Jegatheesan, (2018). Preparation, characterisation and critical flux determination of graphene oxide blended polysulfone (PSf) membranes in an MBR system. *Journal of Environmental Management*, 168-179.
- J. Lu, G. Zhang, H. Zhang, C. Zhao, F. Yang, (2018). Improvement of antifouling performances for modified PVDF ultrafiltration membrane with hydrophilic cellulose nanocrystal. *Applied Surface Science*, 1091-1100.

- J. W. Wang, M. H. Hon, (2004). Biodegradation behaviour and cytotoxicity of composite membrane composed of B-dicalcium pyrophosphate and glucose mediated (polyethylene glycol/chitosan). *Journal of material science*, 129-136.
- J. Y. Chong, B.W. Cecilia, M. K. Li, (2018). Dynamic microstructure of graphene oxide membranes and the permeation flux. *Journal of Membrane Science*, 385-392.
- J.W. Wang, Y.M. Kuo, (2007). Preparation of fructose-mediated (polyethylene glycol/chitosan) membrane and adsorption of heavy metal ions. *Journal of applied science of polymer*, 1480-1489.
- L. Y. Ng, C. P. Leo, A. W. Mohammad, (2011). Optimizing the incorporation of silica nanoparticles in polysulfone/poly(vinyl alcohol) membranes with response surface methodology. *Journal of Applied Polymer Science*, 1804-1814.
- L.F. Fang, L. Cheng, S. Jeon, S.Y. Wang, T.Takahashi, H. Matsuyama, (2018). Effect of the supporting layer structures on antifouling properties of forward osmosis membranes in AL-DS mode. *Journal of Membrane Science*, 265-273.
- M. Padaki, A. M. Isloor, P. Wanichapichart, A. F. Ismail, (2012). Preparation and characterization of sulfonated polysulfone and N-phthaloyl chitosan blend composite cation-exchange membrane for desalination. *Desalination*, 42-48.
- M. S. Jyothi, S. Yadav, G. Balakrishna, (2018). Effective recovery of acids from egg waste incorporated PSf membranes: A step towards sustainable development. *Journal of Membrane Science*, 227-235.
- M. S. Sangeetha, A. Kandaswamy, A. Vijayalakshmi, (2016). Preparation and characterisation of flat sheet micro/nanoporous membranes using polysulfone blend with PVP/PEG and chitosan/chitosan nanoparticles for biomedical applications. *Optoelectronics and Biomedical Materials*, 81-87.
- M. S. Suleman, K.K. Lau, Y.F. Yeong, (2016). Characterization and performance evaluation of PDMS/PSF membrane for CO<sub>2</sub>/CH<sub>4</sub> separation under the effect of swelling. *Procedia Engineering*, 176-183.
- R. Kumar, A. M. Isloor, A.F. Ismail, S. A. Rashid, T. Matsuura, (2013a). Polysulfone-chitosan ultrafiltration membranes: preparation, characterization, permeation, and antifouling properties. *RSC Advanced*, 7855-7861.
- R. Kumar, A. M. Isloor, A.F. Ismail, S.A. Rashid, A. A. Ahmed, (2013c). Permeation, antifouling and desalination performance of TiO<sub>2</sub> nanotube incorporated PSF/CS blend membranes. *Desalination*, 76-84.
- R. Kumar, A. M. Isloor, A.F. Ismail, T. Matsuura, (2013b). Synthesis and characterization of novel water soluble derivative of chitosan as an additive for polysulfone ultrafiltration membrane. *Journal of membrane science*, 140-147.
- R. Kumar, A.M. Isloor, A.F. Ismail, (2014). Preparation and evaluation of heavy metal rejection properties of polysulfone/chitosan, polysulfone/N-succinyl chitosan and polysulfone/N-propylphosphonyl chitosan blend ultrafiltration membranes. *Desalination*, 102-108.
- R. Kumar, A.M. Isloor, A.F. Ismail, T. Matsuura, (2013d). Performance improvement of polysulfone ultrafiltration membrane using N-succinyl chitosan as additive. *Desalination*, 1-8.
- S. Hamzah, Nora'aini, M.M. Ariffin, A.Ali, A.W. Mohammad, (2014). high performance of polysulfone ultrafiltration membrane: effect of polymer concentration. *ARPJ Journal of engineering and applied science*, 2543-2550.
- Y. Zhang, Z. Jin, X. Shan, J. Sunarso, P. Cui, (2010). Preparation and characterization of phosphorylated Zr-doped hybrid silica/PSF composite membrane. *Journal of Hazardous Material*, 390-395.
- Z. Lin, C. Hu, X. Wu, W. Zhong, M. Chen, Q. Zhang, A. Zhu, Q. Liu, (2018). Towards improved antifouling ability and separation performance of polyethersulfone ultrafiltration membranes through poly(ethylenimine) grafting. *Journal of Membrane Science*, 125-133.
- Z. Xu, J. Liao, H. Tang, N. Li, (2018). Antifouling polysulfone ultrafiltration membranes with pendent sulphonamide groups. *Journal of Membrane Science*, 481-489.